FLUSTER: A combined multiecho radial/Cartesian encoded gradient echo sequence for bone and soft tissue segmentation

A. J. van der Kouwe[1,2], T. Benner[1,2], M. Hamm[3], S. Nielles-Vallespin[4], and B. Fischl[5,6]

[1]Athinoula A. Martinos Center for Biomedical Imaging, Massachusetts General Hospital, Charlestown, MA, United States, [2]Department of Radiology, Harvard Medical School, Brookline, MA, United States, [3]Siemens Medical Solutions USA Inc., Charlestown, MA, United States, [4]Siemens Healthcare, Erlangen, Germany, [5]Department of Radiology, Massachusetts General Hospital, Charlestown, MA, United States, [6]CSAIL, Massachusetts Institute of Technology, Cambridge, MA, United States

Introduction and Background

While fully automated methods for MR-based *brain* morphometric analysis are well established [1], tools for automated *whole head* segmentation are not available. This is partly due to the additional contrasts required in the images - in particular the morphometry sequences are usually insensitive to bone, and fat is ignored or suppressed. For brain morphometry, we routinely use a sequence that yields good gray/white matter contrast (e.g. MPRAGE [2]) or sequences from which T1/PD can be estimated (e.g. multiple flip angle FLASH with DESPOT1 [3]). For imaging bone, a dual-echo radially encoded gradient echo sequence with ultrashort first echo may be used. To identify fat and water we use multiecho gradient echo sequences. Here we present a multiecho combined radial/Cartesian encoded spoiled gradient echo sequence with the potential to acquire the information needed for whole head segmentation in one or two scans.

Figure 1: Short T2* components (top left), and analysis results of IDEAL run on FLUSTER data (top right: water; bottom left: fat; bottom right: B0 map.

Methods and Results

The FLUSTER (FLASH with additional Ultrashort TE Readouts) sequence is a 3D encoded conventional RF and gradient spoiled sequence with the standard multiple Cartesian encoded gradient echoes. This sequence has an additional radially encoded FID following the excitation with minimum TE of 70 μs. One or more mono- or bipolar radially encoded echoes may also be inserted before the Cartesian echoes. As the radial readouts are typically high bandwidth, one or two may be inserted with little effect on the Cartesian echo times and total acquisition time.

We tested FLUSTER on a Siemens 1.5 T Avanto using the 12-channel head matrix coil. We collected two whole head FLUSTER scans with flip angles of 5° and 30°(2 UTE echoes (TE = 0.07/2.4 ms) at 2298 Hz/px, 2 mm³; 4 Cartesian monopolar echoes (TE = 6.66/10.05/13.45/16.85 ms) at 651 Hz/px, 1.0 x 1.0 x 1.3 mm³; TR 20 ms, sagittal, 10:55 min:s). We subtracted the magnitude images of the first two radial echoes of the 5° scan to obtain the short T2*/bone image, of which a slice is shown in Figure 1. We applied the T2* IDEAL algorithm [4] to the four Cartesian echoes. This algorithm uses an iterative method to estimate a "complex field map" incorporating R2* and ΔB0, together with separate water and fat images. Representative images are shown in Figure 1.

Figure 2: T1 (left) and PD (middle) parameter maps from two FLUSTER acquisitions with 5° and 25° flip angles, and segmentation (right) with cortical surfaces generated by FreeSurfer using the synthetic optimal contrast volume generated from the parameter maps.

We used FreeSurfer [1] to estimate PD and T1 from the four Cartesian echoes from the two scans with different flip angles using an approach similar to DESPOT1 [3]. T2* can also be estimated, but the fit is noisy due to the small TEs. We synthesized a volume with optimal gray/white matter contrast from these parameter estimates and used FreeSurfer to find the cortical surfaces and label the subcortical structures. The results are shown in Figure 2.

Identifying bone from the radial FID/echoes is confounded by the tradeoff between SNR and resolution. Acquisition time becomes excessive at higher resolutions (±1.5 mm isotropic). The UTE image on the right of Figure 3 was acquired in 8 x 3:17 (26:16) min:s (TE 70 μs/4 ms, TR 6 ms, FA 10°, 32768 projections, T_{dwell} 1.7 μs, 8 channel coil, 3T TIM Trio) while the 200 μm CT scan required 20 s (Siemens Volume CT, 120 kV/50 mA). At lower resolutions, voxels representing thin structures like skull overlap adjacent tissue containing water and/or fat. In order to disambiguate bone from water and fat, we fit the parameters of this model to the data (*w*: water fraction, *f*: fat fraction, Δ*f*: fat-water shift, T_E: echo time, R₂*: relaxation rate):

Figure 3: High-resolution (200 μm) CT scan (left) and high-resolution (±1.5 mm) MR UTE scan (right) of skull.

$$s(T_E) = (we^{-R^*_{2|w}T_E} + fe^{(-R^*_{2|f}T_E + i2\pi\Delta f)*T_E})e^{i(\Psi T_E + \Phi)}$$

Using this approach we fitted the model to the 6 radial echoes of a FLUSTER scan of the knee collected on a 3T TIM Trio (TE 70 μs/1.04/1.9/2.76/3.62/4.48 ms radial and TE 6.98/9/11.02/13.04 ms Cartesian, TR 15 ms, FA 14°, 8192 projections, T_{dwell} 1.7 μs, T_{acq} 2:03 min:s). We segmented water and fat by thresholding the signals resulting from the model. We identified bone as tissue for which the signal in the first echo fell within a range of values while the signal from the second echo fell below a threshold. Figure 4 shows an axial slice through the femur above the knee (second echo, left) with the resulting segmentation (right). The red ring outside the knee is the result of low signal blurring in the image resulting from the FID and is less conspicuous in higher-resolution images.

Conclusion

Multiecho FLUSTER provides sufficient information for whole brain morphometry in one or two acquisitions, as well as information for skull cortical bone and fat segmentation. However, accurate detection of bone, especially trabecular bone, may require longer acquisitions or special imaging techniques not yet practical in human imaging [5] to disambiguate the matrix from other contributing components. Reliable fully automated bone detection requires further work.

Acknowledgement

References

[1] Fischl B et al. Neuron 2002; 33:341-355. [2] Van der Kouwe AJW et al. NeuroImage 2008; 40(2):559-569. [3] Deoni et al. Magn Reson Med 2003; 49:515-526. [4] Yu et al. J Magn Reson Imaging 2007; 26:1153-1161. [5] Wu et al. Magn Res Med 2007; 57:554-567.
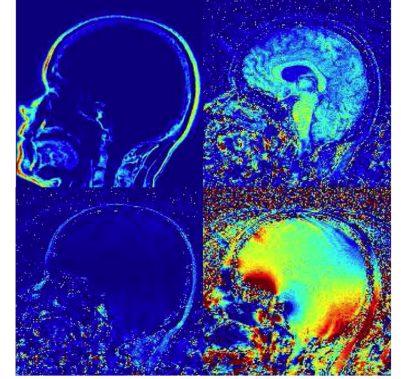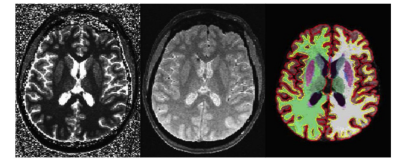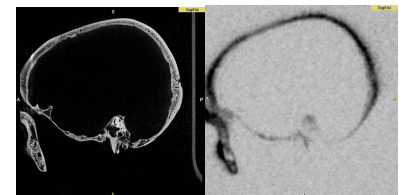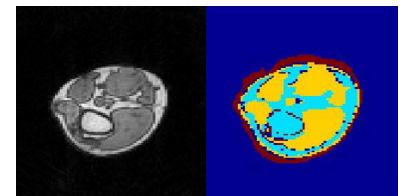
Figure 4: Radially acquired axial slice above knee (left) and segmentation (right). Yellow: water; cyan: fat; red: bone; blue: background.